# Both lamin A and lamin C mutations cause lamina instability as well as loss of internal nuclear lamin organization.

**Document status and date:**
Published: 01/01/2005

**DOI:**
10.1016/j.yexcr.2004.11.020

**Document Version:**
Publisher's PDF, also known as Version of record

**Please check the document version of this publication:**

• A submitted manuscript is the version of the article upon submission and before peer-review. There can be important differences between the submitted version and the official published version of record. People interested in the research are advised to contact the author for the final version of the publication, or visit the DOI to the publisher's website.
• The final author version and the galley proof are versions of the publication after peer review.
• The final published version features the final layout of the paper including the volume, issue and page numbers.
**Link to publication**

Download date: 07 May. 2024

# Both lamin A and lamin C mutations cause lamina instability as well as loss of internal nuclear lamin organization

Jos L.V. Broers[a,b,*], H.J.H. Kuijpers[a], C. Östlund[c], H.J. Worman[c], J. Endert[a], F.C.S. Ramaekers[a]

[a]Department of Molecular Cell Biology, Box 17, Cardiovascular Research Institute Maastricht (CARIM),
University of Maastricht, PO Box 616, NL-6200 MD Maastricht, The Netherlands
[b]Department of Biomedical Engineering, Biomechanics and Tissue Engineering Eindhoven University of Technology, The Netherlands
[c]Departments of Medicine and of Anatomy and Cell Biology, College of Physicians and Surgeons, Columbia University, New York, NY 10027, USA

## Abstract

We have applied the fluorescence loss of intensity after photobleaching (FLIP) technique to study the molecular dynamics and organization of nuclear lamin proteins in cell lines stably transfected with green fluorescent protein (GFP)-tagged A-type lamin cDNA. Normal lamin A and C proteins show abundant decoration of the inner layer of the nuclear membrane, the nuclear lamina, and a generally diffuse localization in the nuclear interior. Bleaching studies revealed that, while the GFP-tagged lamins in the lamina were virtually immobile, the intranuclear fraction of these molecules was partially mobile. Intranuclear lamin C was significantly more mobile than intranuclear lamina A.

In search of a structural cause for the variety of inherited diseases caused by A-type lamin mutations, we have studied the molecular organization of GFP-tagged lamin A and lamin C mutants R453W and R386K, found in Emery–Dreifuss muscular dystrophy (EDMD), and lamin A and lamin C mutant R482W, found in patients with Dunnigan-type familial partial lipodystrophy (FPLD). In all mutants, a prominent increase in lamin mobility was observed, indicating loss of structural stability of lamin polymers, both at the perinuclear lamina and in the intranuclear lamin organization. While the lamin rod domain mutant showed overall increased mobility, the tail domain mutants showed mainly intranuclear destabilization, possibly as a result of loss of interaction with chromatin. Decreased stability of lamin mutant polymers was confirmed by flow cytometric analyses and immunoblotting of nuclear extracts.

Our findings suggest a loss of function of A-type lamin mutant proteins in the organization of intranuclear chromatin and predict the loss of gene regulatory function in laminopathies.
© 2004 Elsevier Inc. All rights reserved.

*Keywords:* Lamin-GFP; Laminopathies; Fluorescence loss of intensity after photobleaching; Vital imaging

## Introduction

The development of green fluorescent protein (GFP) technology in recent years has boosted the use of bleaching techniques, including the commonly used fluorescence recovery after photobleaching (FRAP) and fluorescence loss of intensity after photobleaching (FLIP) techniques [1,2].

Bleaching techniques can be pivotal for the characterization of the molecular organization of fluorescent molecules. If alterations in bleaching behavior are encountered, a change in polymerization or a change in association with other molecules is especially likely.

Nuclear lamins are proteins organized into a fibrous network at the inner layer of the nuclear membrane. Therefore, it is suggested that lamins play a key role in providing structural support to the nuclear membrane. Next to the ubiquitously expressed B-type lamins, lamins B1 and B2 [3,4], most highly differentiated cells express A-type lamins. These proteins, lamin A, lamin AΔ10, and lamin C, are

* Corresponding author. Department of Molecular Cell Biology, Box 17, University of Maastricht, PO Box 616, NL-6200 MD Maastricht, The Netherlands. Fax +31 43 3884151.
*E-mail address:* jos.broers@molcelb.unimaas.nl (J.L.V. Broers).

encoded by the A-type lamin (*LMNA*) gene [5,6]. In addition to perinuclear lamins, lamins can be found in intranuclear regions as tubule-like structures as well as in a fine veil-like network [7,8]. Their interaction with heterochromatin suggests an important function in the maintenance of chromatin organization and gene transcription (for a recent review, see Ref. [9]). Yet, their importance in these processes is still a matter of debate, despite the increased knowledge of the function of these proteins. While the discovery of A-type lamin mutations (causing laminopathies) as well as the generation of A-type lamin knockout mice has provided some insight into their function, the complexity of clinical symptoms simultaneously raised several additional functional questions.

Mutations in the lamin A/C gene (*LMNA*) appear to be responsible for at least eight inherited disorders, including the autosomal form of Emery–Dreifuss muscular dystrophy (EDMD), limb girdle muscular dystrophy, Dunnigan-type familial partial lipodystrophy (FPLD), dilated cardiomyopathy, mandibuloacral dysplasia, Charcot–Marie–Tooth disorder type 2, and two types of Progeria, Hutchinson–Gilford Progeria and atypical Werner syndrome [9–11]. In addition, the combination of Lamin A and ZMPSTE24 defects has been shown to cause restrictive dermatopathy [12]. The relation between *LMNA* mutations and the development of these different diseases is unclear. Potentially, disturbed functions include a diminished mechanical support for the nuclear membrane, which would lead to nuclear fragility. Alternatively, disrupted chromatin organization could alter gene expression and even DNA replication characteristics.

At the nuclear membrane level, the absence of A-type lamins appears to induce structural changes, including the loss of emerin, and nesprin 1α from the nuclear membrane [13,14]. However, studies on abnormalities in cells from (heterozygous) mutant patient material or cells transfected with mutant lamins yielded partly contradictory results. For instance, while some studies could find no nuclear abnormalities in nuclei of cells transfected with R482W A-type lamin mutants [15,16], others [17] did see clear nuclear abnormalities in fibroblast cells from patients with this mutation.

In order to study nuclear lamina organization in affected cells, we have generated GFP-A-type lamin constructs with point mutations identical to those seen in patients. Cells were transfected with these constructs and the integrity of the GFP-lamin polymers was examined using the FLIP technique in living cells. We chose to examine two different *LMNA* mutations occurring in the autosomal form of EDMD, R386K and R453W [18,19], and a *LMNA* mutation, R482W, characteristic for patients with FPLD [20,21]. The R386K mutation is in the rod domain of lamin A/C, while the other two mutations are localized in its tail domain [22]. While the effects of several of these mutations on lamina organization were already studied previously [15–17,23,24], these studies did not examine the

effect on internally localized lamins. Moreover, this is the first study that examines the feasibility of FLIP to study organization of lamins at the molecular level. In order to avoid artefacts due to transfection and overexpression, we chose to examine exclusively cell lines stably transfected with GFP-tagged mutant A-type lamins, with GFP-lamin expression levels similar to native A-type lamins. The use of the "old" temperature-sensitive GFP vector ps65T-C1, permitting a controlled expression of lamin-GFP during only a limited period of time [25], can avoid the occurrence of structural nuclear abnormalities as seen in cells transfected with lamin-EGFP [23].

Based on FLIP and supported by conventional cellular extraction methods, it become obvious that most mutant lamins studied are more loosely organized, both in the lamina and in intranuclear areas.

## Materials and methods

### Mutant constructs

cDNA-encoding prelamin A [26] was cloned into the ps65T-C1 vector (Clontech Laboratories, Inc., Palo Alto, CA) to generate plasmid constructs encoding lamin A-GFP. Lamin C-GFP was generated as described previously [8].

cDNAs encoding mutant forms of lamin A and C were made using the Transformer™ Site-Directed Mutagenesis Kit (Clontech) following the manufacturer's instructions. R386K and R453W are identified in patients with autosomal-dominant EDMD [18,19]; while R482W is found in patients with FPLD [20,21].

### Transfection

CHO-K1 cells were transfected overnight with mutant constructs using DOTAP (Roche Diagnostics, Almere, The Netherlands) according to the manufacturer's instructions. After selection for stable transfectants by geneticin (G418, 500 μg/ml, Gibco-Invitrogen Life Technologies, Carlsbad, CA, USA), cells were subcloned to single-cell colonies by limited dilution. GFP-expressing colonies were selected using an inverted fluorescence microscopy and used for further experiments. Comparison of cells transfected with A-type lamin EGFP or with A-type lamins in pS65T-C1 showed that clones generated with the former construct showed significantly more nuclear abnormalities, including formation of multinucleated cells, prominent nuclear enlargement and folding, and indentation of the nuclear membrane (data not shown). Therefore, no EGFP-tagged lamins were examined further.

### FLIP

Fluorescence intensity in living cells was measured using a MRC600 confocal microscope (BioRad, Hemel

Hempstead, UK), equipped with an air-cooled Argon–Krypton mixed gas laser and mounted onto an Axiophote microscope (Zeiss), using an oil-immersion objective (40×, NA = 1.3). The laser-scanning microscope was used in the dual parameter set-up, according to the manufacturer's specifications, using dual wavelength excitation at 488 and 568 nm. Emission spectra were separated by the standard sets of dichroic mirrors and barrier filters. Comos software (BioRad) was used for bleaching setup. Cells grown on glass coverslips for at least 2 days were exposed to a bleaching regimen, consisting of prebleach recording, bleaching, and post-bleach recording.

In the prebleach recording phase, the central optical slice of a nucleus was determined and a picture was recorded in the Kalman filtering mode (five scans) with a laser setting of 1% of full laser power. To obtain optimal bleaching, scanning was performed at a 30× zoom (vertical box recording setting, i.e., 368 × 512 pixels), in our system is equivalent to scanning a rectangular area of 5 × 7.5 μm. This area was exposed to a repetitive series (15×) of 10 bleaching scans at fast (F3) scan speed at full laser power (100%). The interval between the start of each bleaching round was set at 15 s. As a result, duration of the complete bleaching regimen was approximately 230 s. This bleaching regimen is capable of bleaching all free mobile fluorescent molecules within a cell, as determined by bleaching cells transfected with the ps65T-C1 vector (encoding GFP only), and by bleaching the fluorescence of A-type lamin-GFP in mitotic cells. In fact, most mitotic cells showed no longer fluorescence already after 10 rounds of bleaching (data not shown). The bleaching series was immediately followed by a postbleach recording with settings identical to the prebleach recordings.

Fluorescence intensities of selected cellular regions before and after bleaching were compared with NIH Image software (version 1.62, Wayne Rasband, National Institutes of Health, USA). Identical regions in cells before and after bleaching were selected and the mean fluorescence intensity expressed in pixel values (1–256) was measured in these regions. The relative loss of intensity was calculated for each region after background subtraction. For each cell average intensities were measured for the following areas: lamina (nuclear membrane), intranuclear area without any visible structures, intranuclear tubules (if present), nucleolus (if visible), background area, and bleached areas (only after bleaching). In all recording, the intensity measured in the bleached area corresponded to the background signal.

From each subclone of a particular mutant, 10–15 cells were chosen with an average fluorescence intensity and subjected to the FLIP regimen. Cells with very brightly fluorescent intranuclear aggregates were excluded, as well as cells with fluorescence intensity too low to correct for background variations.

## Preparations of whole cell lysates

Cells were cultured in 75-cm$^2$ tissue culture flasks (Costar, Corning Costar Europe, Badhoevedorp, The Netherlands). Cells were detached by trypsin and after centrifugation the pellet was resuspended in ice-cold lysis buffer (containing 62.5 mM Tris–HCl, pH 6.8, 12.5% glycerol, 2% NP40, 2.5 mM phenylmethylsulphonyl chloride (PMSC), 1.25 mM EDTA, 12.5 μg/ml leupeptin, and 116 μg/ml aprotinin). Next, cell suspensions were incubated on ice for 30 min, dissolved (1: 1) in SDS-sample buffer, boiled for 5 min, and then frozen at −20°C until use in immunoblotting.

## Nuclear extraction studies

Cells were resuspended by trypsin treatment and extracted using 0.5% Triton X-100 in CSK buffer (10 mM PIPES; pH 7.0; 100 mM NaCl; 300 mM sucrose; 3 mM MgCl$_2$; 1 mM EGTA containing 0.5 mM PMSC) for 7 min at 0°C, followed by Dnase I treatment (2 μg/ml DNAse, 30 min at RT). Next, cytoskeletal proteins were extracted by 2 mg/ml sulpho-NHS-acetate in CSK-buffer; 20 min at room temperature, which allows the removal of DNA attached to nuclear scaffold proteins concurrently with proteins attached to DNA and not to the nuclear scaffold [27]. This reaction was stopped by the addition of 10 mM glycine, followed by fixation in 4% formaldehyde in PBS, containing 1% BSA. Fluorescence intensity of different fractions of these cellular remnants (no extraction, extraction with Triton X-100 only, and extractions followed by sulpho-NHS treatment) was measured by flow cytometric analysis. Flow cytometric analyses were performed essentially as described [28]. Different fractions of lamin GFP-transfected cells were analyzed using a FACSort flow cytometer and Cellquest analysis software (Becton Dickinson, Sunnyvale, CA). Excitation was done at 488 nm and emission was detected using a 515- to 545-nm bandpass filter.

For immunoblotting, nucleo-cytoskeletal fractions were prepared as follows: cells were rinsed with ice-cold PBS and then harvested by scraping in ice-cold RSB buffer containing 10 mM Tris–HCl, pH 7.4, 10 mM NaCl, 1.5 mM MgCl$_2$, and 0.5 mM PMSC. Next, the cell suspension was extracted in 0.5% Triton X-100 in RSB buffer for 10 min on ice, followed by incubation in buffer containing 1 μg/ml DNase I (Sigma), 50 μg/ml RNase A (Sigma), 10 mM Tris–HCl, pH 7.4, 110 mM NaCl, 1.5 mM MgCl$_2$, and 0.5 mM PMSC, for 20 min at RT. Next, cells were exposed to high salt extraction (500 mM NaCl in PBS) for 20 min at room temperature. Finally, after washing with RSB buffer, the pellet was dissolved 1:1 in SDS sample buffer, boiled for 5 min, and stored at −20°C for gel electrophoresis.

Gel electrophoresis and immunoblotting were performed as described previously [29]. After blocking in 0.5% Triton X-100/PBS buffer containing 3% nonfat dry milk, cells were incubated with mouse antibody JOL2 (IgG1; dilution 1:50). This antibody reacts with an epitope

(amino acids 464–572) in the C-terminal domain of lamin A, AΔ10, and C [30]. A secondary antibody peroxidase-conjugated rabbit anti-mouse Ig (DAKO A/S, Glostrup, Denmark) was used. Peroxidase activity was detected by chemiluminescence (Pierce, Rockford, IL, USA). Finally, RX Fuji medical X-ray films (Fuji, Tokyo, Japan) were used for the visualization of luminescent signals.

## Results

### Altered localization of mutated GFP lamins

In contrast to some previously published papers, we chose to examine the nuclear localization of lamins and nuclear membrane-related proteins in stably transfected, cloned cell lines only. Subclones with apparent normal nuclear localization were selected and used for further analyses. While for each mutant a spectrum of intranuclear localization pattern was observed, this spectrum was retained within most of the subclones. Therefore, only one subclone for each mutant was chosen for analysis. Fig. 1 shows representative cells from transfections with wild-type (wt) lamin A-GFP, wt lamin-C-GFP, and mutant clones. Both in normal and in mutant clones it is clear that lamin C-GFP shows more intranuclear signal than lamin A-GFP (compare panels A and B).

Characteristic for the lamin A-R386K-GFP (Figs. 1A3 and A4) and lamin C-R386K-GFP (Figs. 1B3 and B4) mutants was the observed change in ratio between the nuclear membrane and the nuclear interior. Compared with wt lamin A or C transfected cells, relatively more signal was observed in intranuclear areas, mainly seen as a diffuse intranuclear labeling. The bright intranuclear fluorescence almost completely masks the lamina fluorescence, which only becomes clearly visible after bleaching (Fig. 2). Furthermore, these mutants displayed the absence of fluorescent intranuclear tubules.

Comparison of lamin A R453W-GFP (Figs. 1A5 and A6) and lamin C R453W-GFP (Figs. 1B5 and B6) with wt lamin A or lamin C-GFP showed subtle alterations in localization of the transfected protein, both in the ratio between nuclear membrane and nuclear interior fluorescence. Careful examination of transfected cells with confocal microscopy showed irregular fluorescence distribution along the nuclear rim and even sometimes a pronounced absence of lamin A R453W-GFP and lamin C R453W-GFP in particular nuclear membrane areas (Fig. 1A5, arrow; 1B5 and B6, arrow). This pattern was only rarely observed in wt lamin A- or C-transfected cells. In addition, fluorescence signal was often very pronounced in irregular intranuclear aggregates. Tubular structures extending from the nuclear membrane into the nuclear interior were not observed. Most cells appear to have a reduced level of diffuse lamin labeling in intranuclear lamins.

Lamin A R482W-GFP (Figs. 1A7 and A8) patterns were very similar to lamin A 453W-GFP mutants, i.e., an uneven distribution over the nuclear membrane, with locally complete absence of fluorescence (Fig. 1A7, arrow) and the presence of highly irregular intranuclear aggregates. Cell lines of the R482W mutant showed a striking difference between lamin A R482W-GFP and lamin C R482W-GFP uptake in the nucleus in part of the cells. In the lamin C R482W-GFP transfectant (Figs. 1B7 and B8), some GFP signal can be seen as a diffuse fluorescence outside of the nucleus. Moreover, the intense, diffuse labeling of the nuclear interior of these cells completely covers the characteristic nuclear rim labeling in some cells. In other cells, pronounced intranuclear tubular structures were seen, with a much more irregular appearance than wt cells.

### Fluorescence loss of intensity after photobleaching

Characteristic bleaching behaviors for normal and mutant A-type lamins are shown in Figs. 2A–D. Average percentages of fluorescence retained after photobleaching in denoted areas are shown in Figs. 3A and B. Comparison of normal lamin A-GFP with lamin C-GFP showed that both proteins had almost identical bleaching characteristics at the nuclear rim (loss in lamina intensity) with an average retention of 95% and 88%, respectively (Figs. 2A and 3A). The same held true for intranuclear tubules, which appeared to be similarly stable (calculations not shown), and for diffuse intranuclear areas (Fig. 3B).

In contrast, an increased solubility of intranuclear (diffuse) fluorescence was observed in lamin C-GFP-transfected cells (retainment 88% vs. 55%, respectively; Figs. 2A and B). While lamin C-GFP showed more diffuse intranuclear lamins, these proteins appeared to be significantly more mobile than lamin A-GFP. Strikingly, intercellular variation in fluorescence retainment in lamin C-GFP-transfected cells was much larger than lamin A-GFP-transfected cells, ranging from 20% to 80% retainment in the internal nucleus.

The R386K mutant is characterized by the large loss of fluorescence both in the lamina and in intranuclear areas (Fig. 2B). Only about half of the fluorescence intensity of lamin A R386K-GFP (54%) is retained in the lamina after bleaching, while in intranuclear areas 20% is retained. An even more dramatic decrease of signal is observed in the lamin C R386K-GFP mutant with an almost complete loss of mutant lamin C fluorescence both in the lamina and in intranuclear areas (retainment of 7% and 2%, respectively) after photobleaching. In several lamin C R386K-GFP-transfected cells, no lamina signal at all was retained after bleaching, indicating that this mutant seems to have lost most of its capability to participate in a structural lamin network. Bleaching of the other two mutants revealed more subtle differences in bleaching behavior. Calculations of the loss of intensity in the lamina showed that lamin A R453W-GFP did integrate
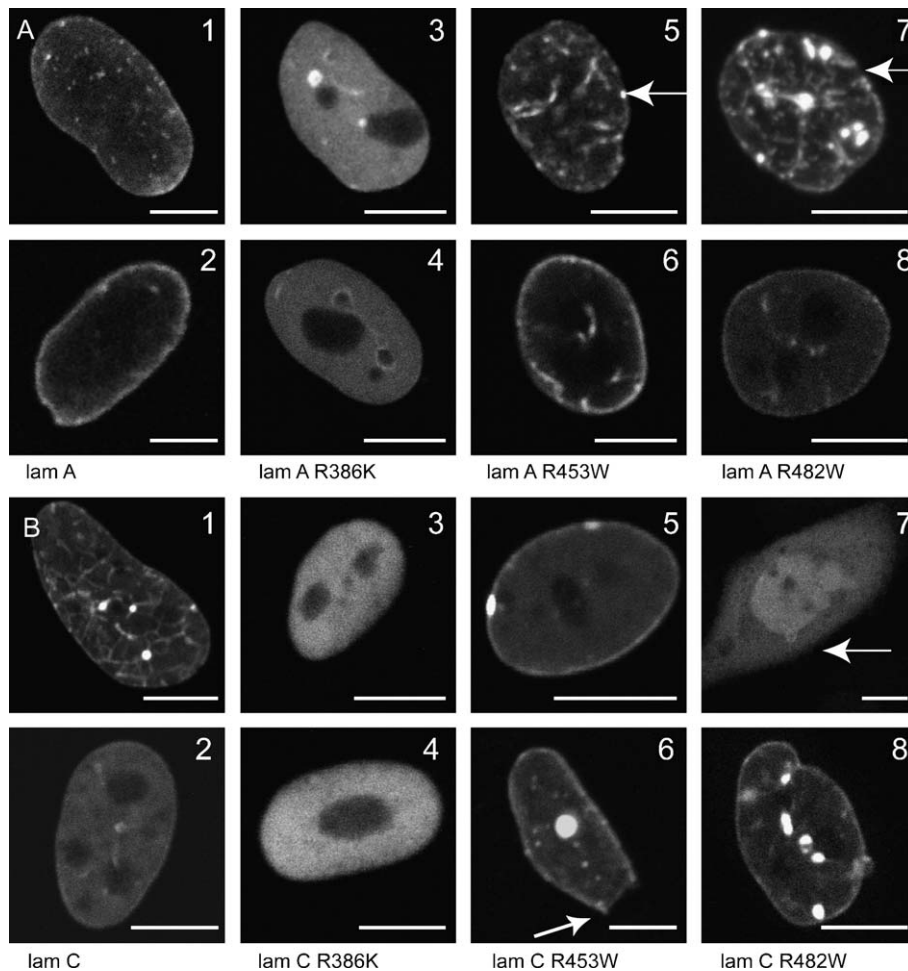
Fig. 1. Comparison of fluorescence patterns in CHO-K1 cells stably transfected with A-type lamin-GFP. (A) Lamin A-GFP and lamin A-GFP mutants. Wild-type (wt) lamin A-GFP shows an evenly GFP-decorated nuclear lamina, modest amounts of intranuclear lamins, and variable amounts of intranuclear tubules (A1 and A2). The lamina A R386K-GFP mutant shows much more diffuse intranuclear labeling, with only occasional intranuclear tubules (A3 and A4). The lamin A R453W-GFP (A5 and A6) and lamin A R482W-GFP (A7 and A8) mutants showed similar patterns with irregular decoration of lamins at the nuclear membrane (arrows) and in the nuclear interior. (B) Lamin C-GFP and lamin C-GFP mutants. Compared to wt lamin A in general, more diffuse intranuclear lamin C can be observed (B1 and B2). In the lamin C R386K-GFP mutant, the decoration of the nuclear membrane cannot be distinguished from the bright diffuse intranuclear labeling (B3 and B4). Note the absence of intranuclear aggregates and tubules in these cells. In the lamin C R453W-GFP mutant, the irregular decoration of the nuclear membrane is striking (B5 and B6, arrow). Pronounced intranuclear aggregates and absence of tubules are characteristic. The lamin C R482W-GFP mutant (B7 and B8) shows variable amounts of this protein in the cytoplasm (arrow). In cells with large amounts of this protein in the cytoplasm, a strongly reduced labeling of tubules and nuclear membrane can be found (B7). However, some cells do show membrane labeling, next to intranuclear aggregation (B8). Scale bars represent 10 μm in all pictures.

quite well into the lamina, and no significant differences with wt lamin A-GFP in bleaching loss were found (Fig. 2C). Still, integration into the intranuclear areas of the cell was significantly decreased ($P < 0.005$, Student's $t$ test). Integration of lamin C R453W-GFP both into the lamina and into intranuclear areas was significantly reduced ($P$ values of 0.003 and 0.005, respectively, Student's $t$ test).

Bleaching of lamin R482W-GFP mutants showed a moderate loss of intensity in the lamina with the lamin A R482W-GFP mutant ($P$ value 0.064 when compared with wt lamin A-GFP, Student's $t$ test), while a very pronounced loss was seen in the lamina with the lamin C R482W-GFP mutant ($P < 0.006$).

Loss of signal in intranuclear areas was much more significant ($P$ values of 0.0001 and 0.003 for lamin A

and C, respectively, Student's $t$ test). Interestingly, the fluorescence signal seen in the cytoplasm of these cells was also lost during bleaching, indicating that these molecules were freely interchangeable between the two compartments (Fig. 2D).

### Biochemical extraction

In order to confirm the increased solubility of most of the mutant lamins investigated, we performed nuclear protein extractions and analyzed them at cellular level by flow cytometric analysis as well as by immunoblotting.

Comparison of fluorescence intensities by flow cytometry (Fig. 4) showed that in all mutants the extraction by Triton X-100 and sulpho-NHS resulted in a relatively
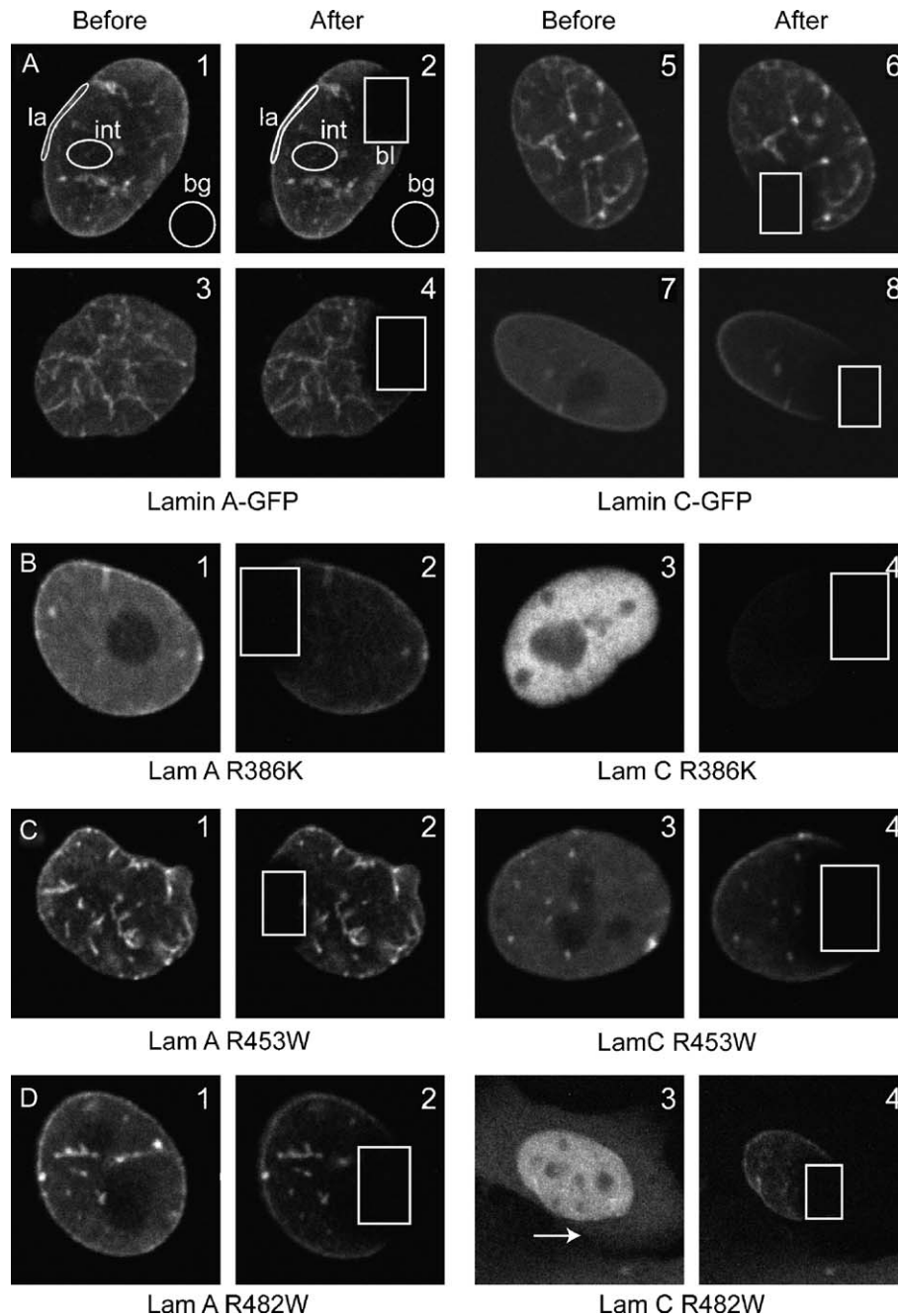
Fig. 2. Fluorescence loss of intensity studies on CHO-K1 cells transfected with wt lamin A-GFP (A1–4), wt lamin C-GFP (A5–8), and the GFP-tagged A-type lamin mutants R386K (panel B), R453W (panel C), and R482W-GFP (panel D). Panels A1 and A2: example of different areas measured in cell before and after photobleaching. la = lamina, int = intranuclear region, bg = background, bl = bleached area. For clarity, only the rectangle of the bleached area is shown in the other panels. Note that bleaching for lamin A has only limited effect on fluorescence intensities outside of bleached region (A1–4). Bleaching of lamin C revealed stable lamina fluorescence in most cells (A5–8) with, however, a significant decrease in intranuclear labeling (A7 and A8). Panel B: note the overall decrease in lamina and intranuclear areas for lamin A R386K-GFP (B1 and B2) and the dramatic decrease to barely detectable levels for the lamin C R386K-GFP mutant (B3 and B4). Panel C: note the stability of lamin A R453W-GFP mutant fluorescence at the lamina and intranuclear aggregates after photobleaching (C1 and C2), while for the lamin C mutant a significant decrease both at the peripheral lamina and the nucleoplasm is observed (C3 and C4). Panel D: loss of fluorescence is limited in the lamina for the lamin A 482W-GFP mutant (D1 and D2), while a considerable loss is seen in the lamin C R482W-GFP mutant (D3 and D4). Note in addition that the cytoplasmic signal in this bleached cell is lost, indicating that these molecules can diffuse rapidly into the nucleus. Cytoplasmic signal from neighboring cells, however, is not affected (arrow).

larger loss of fluorescence as compared with wt lamin-GFP. Fig. 4 shows a comparison of extractions performed with lamin C-GFP and with the three lamin C-GFP mutants. Indeed, in all three mutants, increased extract-ability was observed, with the best retention in the mutant showing the least bleaching in the FLIP studies (lamin C R453W-GFP), and an almost complete loss of fluorescence in the lamin C R386K-GFP mutant, similar

## A    Fraction of fluorescence retained in lamina after photobleaching



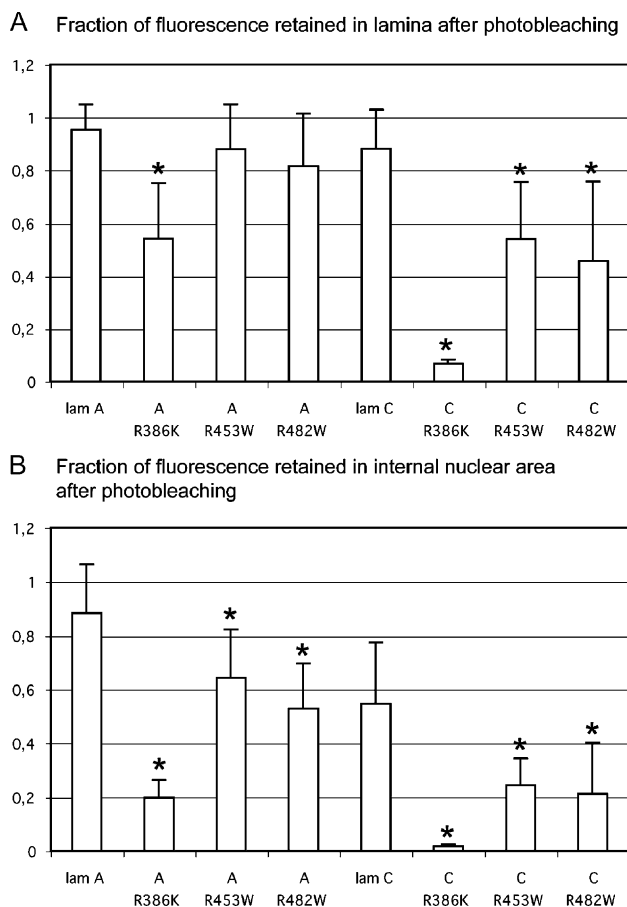## B    Fraction of fluorescence retained in internal nuclear area after photobleaching



Fig. 3. Summary of fluorescence loss of intensity measurements. Mean values of retained fluorescence in the perinuclear lamina (A) and diffuse intranuclear regions (B) are given with standard errors. Statistical analyses were performed using Student's $t$ test, comparing lamin A-GFP with lamin A mutants and lamin C-GFP with lamin C mutants. Asterisks indicate significant ($P < 0.05$) differences.

to the bleaching studies (compare Figs. 2 Figs. 3 Figs. 4). Extraction with sulpho-NHS was performed, since a previous study indicated that this extraction would differentiate between (lamin) molecules associated with DNA in the nucleus and molecules not associated with DNA. Since we suspect that mutant lamin-GFP is less well associated with chromatin than wt lamin-GFP, we expected to find that the additional sulpho-NHS treatment after Triton X-100 extraction would cause more loss of signal in the wt lamin transfected. However, such a distinction could not be found with the cells examined (comparison not shown).

Different extractions on cell populations for immuno-blotting (Fig. 5) showed that mutant GFP-tagged lamins could more easily be extracted from cells than wt GFP-tagged lamins. While lamin C-GFP was largely resistant to Triton X-100 extraction, followed by high-salt treatment, most of the mutant signal (in this case lamin C R482W-GFP) was lost upon extraction by 500 mM NaCl.

## Discussion

In this study, we have compared the molecular organization of different mutant forms of A-type lamin proteins. Integration of lamins into internal nuclear structures can be observed at three distinguishable levels The first and the most prominent level of organization is at the nuclear envelope, where lamins are organized into a thick meshwork of lamin polymers, the nuclear lamina [31]. The exact lamina organization remains unclear, since lamins, in contrast to other intermediate filaments, have only a limited tendency to form filaments in vitro [32]. Yet, it is clear that the lamina is mainly formed by A- and B-type lamins, tightly anchored to the nuclear membrane by several inner nuclear membrane binding proteins, including LAP2 isoforms, the lamin B receptor (LBR), nurim, the MAN antigen, otefin, and emerin [9,33]. Recently, several new inner nuclear membrane proteins have been discovered. These include the ring-finger binding protein RFBP, luma, and the group of nesprin/myne-1 proteins [34] (for a review, see Ref. [35]). The molecular interaction between these lamina-associated proteins and lamins remains obscure. Recent studies indicate that lamins keep the lamina-associated proteins localized to this membrane, rather than the membrane proteins holding lamins. Absence of lamins causes the loss of emerin from the nuclear membrane into the cytoplasm [14]. In addition, nesprin 1alfa becomes mislocalized with emerin to the endoplasmic reticulum in human fibroblast cells lacking A-type lamin expression [13]. Moreover, LAP2 beta as well as lamin B becomes absent from large areas of the nuclear membrane in *LMNA* null cells [13,14] or *LMNA* mutant cell lines [17].

The second level of lamina organization is the presence of prominent intranuclear tubule-like structures, the function of which remains largely unknown. These structures, partly resulting from invaginations of the nuclear membrane and partly consisting of lamins not associated with the nuclear membrane [8,36], penetrate deep into the nucleus and often transverse the complete nucleus, suggesting a potential transport function. Unclear so far is whether these tubule-like structures correspond to some of the intranuclear speckles observed by other groups [37].

The third level of lamina organization is a so-called veil-like [7] network of lamin proteins seen as diffuse internal nuclear fluorescence by immunocytochemistry and GFP tagging of lamins [7,8]. While the resolution of light microscopy is not sufficient to reveal any structure in this veil, it has been shown that there is a molecular organization of these proteins to each other or to other intranuclear structures, since bleaching studies showed that these proteins are only partly freely mobile [7,8]. This level of organization could well represent the intranuclear 10-nm filaments, visible at EM level using specialized nuclear extraction techniques [38]. However, the head and tail of lamins seem to prohibit the typical filament formation [32]. The possible alterations at this level of organization have
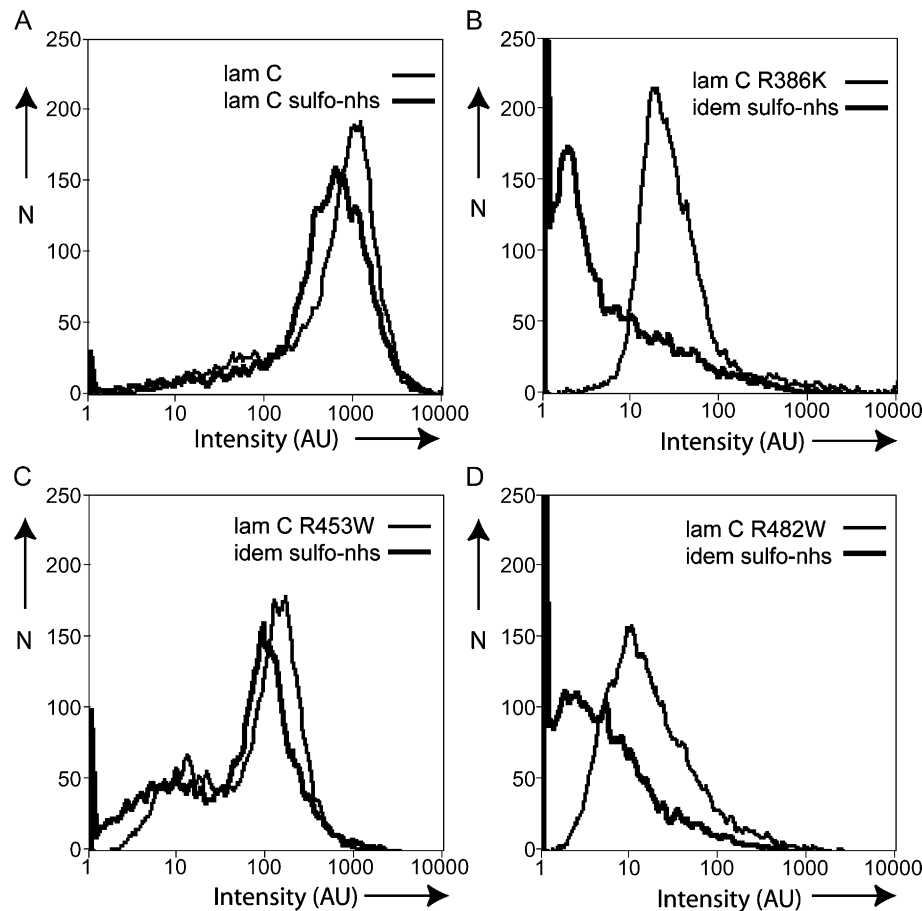
Fig. 4. Flow cytometric analysis of fluorescent signal before and after Triton X-100 and sulpho-NHS extraction. A: wt lamin C-GFP, B: mutant lamin C R386K-GFP, C: lamin C R453W-GFP, D: lamin C R482W-GFP. Note that especially lamin C R386K-GFP fluorescence is susceptible to extraction.

gained our special attention, since it has been stated that lamins could form a framework for transcription regulation [38]. Since most potentially active genes are not localized at the periphery, but in well-defined transcriptional complexes in the nuclear interior [39], one would expect that if lamins have a functional role in this process, they should indeed by localized in these regions. As a consequence, loss of gene regulatory function, as predicted in laminopathies, should be reflected in the loss of intranuclear lamin organization.

Mutations in A-type lamins cause a spectrum of diseases ranging from EDMD to Hutchinson–Gilford progeria and atypical Werner syndrome [40]. Several studies have already shown that most A-type lamin mutations result in nuclear abnormalities, including frequent blebbing or 'herniations', large-scale alterations in nuclear shape, increased separation of the inner and outer nuclear membranes, clustering of nuclear pores, loss of some inner nuclear membrane proteins from one pole of the nucleus, and disruption of the underlying electron-dense heterochromatin. These abnormalities can be observed in cells lacking A-type lamins [13,14,41], in cells from patients with A-type lamin mutations [17,42], and in cells transfected with A-type lamin mutants [15,23,24,43]. However, the extent of these alterations seems to be highly variable,

especially in cultured cells, in which A-type lamin-containing cells are transfected with mutant forms of A-type lamin constructs. Even the effects of the same mutation on nuclear morphology appear to vary. For instance, the R482W or R482Q mutants in FPLD cause no visible abnormalities in A-type lamin localization and association with other nuclear proteins after transient transfection [15,16,24]. However, other studies show nuclear alterations in a minority of cells in cultured fibroblasts from a patient carrying this mutation [17] or the R482L mutation [44]. A major difference between the two systems could be the fact that in all transfection studies performed so far only transiently transfected cells were studied. In order to possibly solve this issue we have generated stable transfectants.

FLIP experiments on normal A-type lamins tagged with GFP confirmed that these proteins are very stably incorporated into the nuclear lamina (see also Refs. [7,8,45]), since these proteins could not be bleached by repetitive bleaching in a nearby area of the nucleus. A considerable amount (up to 90%) of intranuclear lamins, visible as a diffuse fluorescence pattern in GFP-lamin-transfected cells, appeared also immobile. However, about half of the cells transfected with lamin C showed a much higher intranuclear

wt. total    mut. total

lam C(-R482W)-GFP =

lam A =

lam C =

wt. Tx100    wt. +NaCl

lamin C -GFP =

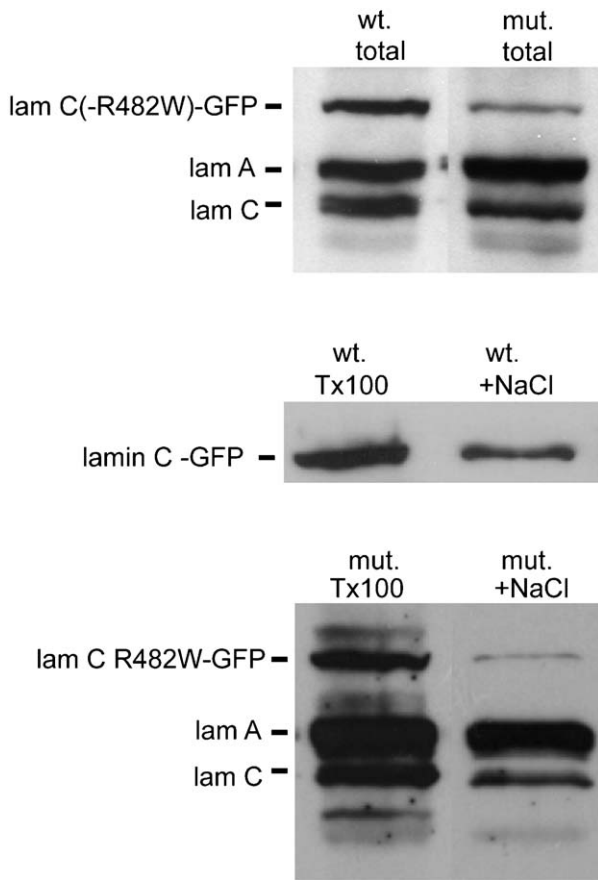mut. Tx100    mut. +NaCl

lam C R482W-GFP =

lam A =

lam C =

Fig. 5. Immunoblotting of total cellular extracts (upper panel) of CHO cells transfected with lamin C-GFP and lamin C R482W-GFP, identifying the lamin C-GFP protein (wt.) or lamin C R482W-GFP (mut.), next to native lamins A and C of CHO-K1 cells. In cells transfected with wt lamin C-GFP (middle panel), the high-salt treatment (+NaCl, right) had only little effect on the intensity compared to lamin C-GFP signal in Triton X-100-extracted cells (Tx100, left). Lower panel: Triton X-100 extraction followed by high-salt extraction of CHO cells transfected with lamin C R482W-GFP resulted in a considerable loss in lamin C R482W-GFP signal (compare left and right lane), while native lamin A and lamin C remained to a large extent present in these extracts.

lamin mobility. These data suggest a dynamic shuttling of lamin C molecules from immobile nuclear complexes into a diffusible nucleoplasmic state. In contrast to previous studies that assigned this more soluble state to the beginning of G1-phase for lamin A(-GFP) [7], we could not find such a correlation for lamin C, nor did we find a relation between mobility levels and other cell cycle phases (data not shown).

Our studies on mutant lamin localization based on confocal fluorescence microscopy alone confirmed most findings of previous studies. However, because of the rigid selection of apparently normal looking clones, we have largely excluded abnormalities due to the transfection and/or integration into the genome. As a result, most mutants we have examined exhibited only limited morphological abnormalities. Clearly the most dramatic structural changes are seen in the R386K-GFP mutant, with a prominent reduced incorporation into the nuclear lamina. R453W-GFP and R482W-GFP mutants showed only limited abnormal-

ities, such as uneven lamina thickness. In addition, the loss of well-structured tubules was notable in all mutants.

Bleaching studies of different mutants did not show a significantly compromised assembly at the level of the lamina for two out of three lamin A mutants compared to wt lamin A. However, all three lamin C mutants showed a decreased ability to stably integrate into the nuclear lamina compared to lamin C. These differences imply a different effect of identical mutations, when they occur either in lamin A or in lamin C, stress the differential behavior of the two lamin proteins, and suggest a different role in the formation of the nuclear lamina. Combined with the known differences in processing between lamins A and C [46], as well as differential levels of expression in differentiated cells [47,48], it is likely that the contribution of each (mutant) lamin to this disorganization will be different.

Mutations in the rod domain of lamin proteins are predicted to have more impact on lamina organization than tail domain mutations, since lamin dimer formation is achieved via the alpha-helical rod domains [49]. While a recent study indicated that most of the known coil-2b A-type lamin mutations, including R386K, do not have a major impact on coiled-coil dimer formation itself, it is suggested that these mutations affect molecular interactions in higher-order filament assembly [49]. Indeed, a previous study showed that mutations in the rod domain affect the assembly of the lamina in transfected LMNA-deficient cells [16]. Our study confirms that the lamin A- and the lamin C R386K-GFP proteins exhibit a pronounced disturbance in lamina association and exhibit the highest mobility as compared to R453W and R482W mutants. These two other mutants, with mutations localized in the carboxy terminal tail region of the molecule, show a more stable nuclear envelope localization. Compared to wild-type lamins, however, these latter two mutants show a compromised association with intranuclear structures. The carboxy terminal region of A-type lamin proteins is known to contain a DNA-binding region and A-type lamin proteins containing the R482Q or the R482W mutation show a 5-fold decrease in affinity to DNA [50]. While nothing is published about the affinity to DNA of the R453W mutant, this mutation does also occur in this DNA-binding region of the A-type lamin proteins (AA 411–553) [50] and could thus affect DNA affinity as well. The increased intranuclear mobility could thus very well reflect the decreased association with DNA in these mutants. From a previous study it was predicted that the R453W and not the R482W mutation destabilizes the A-type lamin carboxy terminal domain structure [22]. These apparent structural differences are not reflected in our bleaching studies, since both mutants behaved essentially similar.

Clearly, more research should be performed to solve this issue. Meanwhile, evidence is accumulating that lamina disorganization causes not only nuclear [51], but also total cellular weakness [52]. In this respect, the absence of tubules in mutant cells could add to the reduced mechanical

stiffness. Whether these tubules do perform a structural support function is not yet shown. Mechanical weakness explains part of the symptoms seen in patients with laminopathies, especially those associated with muscle wasting and muscular weakness, since mechanical weakening of vascular endothelial and smooth muscle cells may be the initial pathological event leading to these symptoms [53]. However, mechanical factors alone do not seem to explain all of the symptoms in these patients, such as severe conduction disturbances, often resulting in sudden heart failure. An explanation for these symptoms could be the loss of gene regulatory functions in these cells. Indeed, in normal cells, the association with the retinoblastoma gene protein [54,55] and with transcription factors SREBP1 [56], BAF [57], and MOK1 [58] was shown. Loss of association with Rb and with SREBP1 was found in *LMNA*−/− cells [41,54]. In this respect, our finding that intranuclear lamins are not correctly assembled into the internal nuclear veil in all of the mutants strongly argues in favor of the loss of other gene regulatory functions in these diseases, in addition to the loss of mechanical stiffness.

In summary, we have analyzed the molecular organization of mutant A-type lamin constructs in stable transfected cell and found disorganization of these proteins at three different levels of organization, each of which could explain different aspects of the clinical symptoms of laminopathies.

# References

[1] J. Lippincott-Schwartz, J.F. Presley, K.J.M. Zaal, K. Hirschberg, C.D. Miller, J. Ellenberg, Monitoring the dynamics and mobility of membrane proteins tagged with green fluorescent protein, in: K.F. Sullivan, S.A. Kay (Eds.), Green Fluorescent Proteins, Methods Cell Biol., vol. 58, Academic Press, San Diego, 1999, pp. 261–281.

[2] J. Ellenberg, J. Lippincott-Schwartz, Dynamics and mobility of nuclear envelope proteins in interphase and mitotic cells revealed by green fluorescent protein chimeras, Methods 19 (1999) 362–372.

[3] G. Biamonti, M. Giacca, G. Perini, G. Contreas, L. Zentilin, F. Weighardt, M. Guerra, G. Della Valle, S. Saccone, S. Riva, A. Falaschi, The gene for a novel human lamin maps at a highly transcribed locus of chromosome 19 which replicates at the onset of S-phase, Mol. Cell. Biol. 12 (1992) 3499–3506.

[4] F. Lin, H.J. Worman, Structural organization of the human gene (LMNB1) encoding nuclear lamin B1, Genomics 27 (1995) 230–236.

[5] F. Lin, H.J. Worman, Structural organization of the human gene encoding nuclear lamin A and nuclear lamin C, J. Biol. Chem. 268 (1993) 16321–16326.

[6] B.M. Machiels, A.H.G. Zorenc, J.M. Endert, H.J.H. Kuijpers, G.J.J.M. van Eys, F.C.S. Ramaekers, J.L.V. Broers, An alternative splicing product of the lamin A/C gene lacks exon 10, J. Biol. Chem. 271 (1996) 9249–9253.

[7] R.D. Moir, M. Yoon, S. Khuon, R.D. Goldman, Nuclear lamins A and B1. Different pathways of assembly during nuclear envelope formation in living cells, J. Cell Biol. 151 (2000) 1155–1168.

[8] J.L.V. Broers, B.M. Machiels, G.J.J. van Eys, H.J.H. Kuijpers, E.M.M. Manders, R. van Driel, F.C.S. Ramaekers, Dynamics of the nuclear lamina as monitored by GFP-tagged A-type lamins, J. Cell Sci. 112 (1999) 3463–3475.

[9] Y. Gruenbaum, R.D. Goldman, R. Meyuhas, E. Mills, A. Margalit, A. Fridkin, Y. Dayani, M. Prokocimer, A. Enosh, The nuclear lamina and its functions in the nucleus, Int. Rev. Cytol. 226 (2003) 1–62.

[10] H.J. Worman, J.C. Courvalin, The nuclear lamina and inherited disease, Trends Cell Biol. 12 (2002) 591–598.

[11] H.J. Worman, J.C. Courvalin, How do mutations in lamins A and C cause disease? J. Clin. Invest. 113 (2004) 349–351.

[12] C.L. Navarro, A. De Sandre-Giovannoli, R. Bernard, I. Boccaccio, A. Boyer, D. Genevieve, S. Hadj-Rabia, C. Gaudy-Marqueste, H.S. Smitt, P. Vabres, L. Faivre, A. Verloes, T. Van Essen, E. Flori, R. Hennekam, F.A. Beemer, N. Laurent, M. Le Merrer, P. Cau, N. Levy, Lamin A and ZMPSTE 24 (FACE-1) defects cause nuclear disorganization and identify restrictive dermopathy as a lethal neonatal laminopathy, Hum. Mol. Genet. 13 (2004) 2493–2503.

[13] A. Muchir, B.G. van Engelen, M. Lammens, J.M. Mislow, E. McNally, K. Schwartz, G. Bonne, Nuclear envelope alterations in fibroblasts from LGMD1B patients carrying nonsense Y259X heterozygous or homozygous mutation in lamin A/C gene, Exp. Cell Res. 291 (2003) 352–360.

[14] T. Sullivan, D. Escalante-Alcalde, H. Bhatt, M. Anver, N. Bhat, K. Nagashima, C.L. Stewart, B. Burke, Loss of A-type lamin expression compromises nuclear envelope integrity leading to muscular dystrophy, J. Cell Biol. 147 (1999) 913–920.

[15] W.H. Raharjo, P. Enarson, T. Sullivan, C.L. Stewart, B. Burke, Nuclear envelope defects associated with LMNA mutations cause dilated cardiomyopathy and Emery–Dreifuss muscular dystrophy, J. Cell Sci. 114 (2001) 4447–4457.

[16] I. Holt, C. Östlund, C.L. Stewart, N. Man, H.J. Worman, G.E. Morris, Effect of pathogenic mis-sense mutations in lamin A on its interaction with emerin in vivo, J. Cell Sci. 116 (2003) 3027–3035.

[17] C. Vigouroux, M. Auclair, E. Dubosclard, M. Pouchelet, J. Capeau, J.C. Courvalin, B. Buendia, Nuclear envelope disorganization in fibroblasts from lipodystrophic patients with heterozygous R482Q/W mutations in the lamin A/C gene, J. Cell Sci. 114 (2001) 4459–4468.

[18] G. Bonne, M.R. Di Barletta, S. Varnous, H.M. Becane, E.H. Hammouda, L. Merlini, F. Muntoni, C.R. Greenberg, F. Gary, J.A. Urtizberea, D. Duboc, M. Fardeau, D. Toniolo, K. Schwartz, Mutations in the gene encoding lamin A/C cause autosomal dominant Emery–Dreifuss muscular dystrophy, Nat. Genet. 21 (1999) 285–288.

[19] G. Bonne, E. Mercuri, A. Muchir, A. Urtizberea, H.M. Becane, D. Recan, L. Merlini, M. Wehnert, R. Boor, U. Reuner, M. Vorgerd, E.M. Wicklein, B. Eymard, D. Duboc, I. Penisson-Besnier, J.M. Cuisset, X. Ferrer, I. Desguerre, D. Lacombe, K. Bushby, C. Pollitt, D. Toniolo, M. Fardeau, K. Schwartz, F. Muntoni, Clinical and molecular genetic spectrum of autosomal dominant Emery–Dreifuss muscular dystrophy due to mutations of the lamin A/C gene, Ann. Neurol. 48 (2000) 170–180.

[20] H. Cao, R.A. Hegele, Nuclear lamin A/C R482Q mutation in Canadian kindreds with Dunnigan-type familial partial lipodystrophy, Hum. Mol. Genet. 9 (2000) 109–112.

[21] S. Shackleton, D.J. Lloyd, S.N. Jackson, R. Evans, M.F. Niermeijer, B.M. Singh, H. Schmidt, G. Brabant, S. Kumar, P.N. Durrington, S. Gregory, S. O'Rahilly, R.C. Trembath, LMNA, encoding lamin A/C, is mutated in partial lipodystrophy, Nat. Genet. 24 (2000) 153–156.

[22] I. Krimm, C. Östlund, B. Gilquin, J. Couprie, P. Hossenlopp, J.P. Mornon, G. Bonne, J.C. Courvalin, H.J. Worman, S. Zinn-Justin, The Ig-like structure of the C-terminal domain of lamin A/C, mutated in muscular dystrophies, cardiomyopathy, and partial lipodystrophy, Structure (Camb.) 10 (2002) 811–823.

[23] C. Favreau, E. Dubosclard, C. Östlund, C. Vigouroux, J. Capeau, M. Wehnert, D. Higuet, H.J. Worman, J.C. Courvalin, B. Buendia, Expression of lamin A mutated in the carboxyl-terminal tail generates an aberrant nuclear phenotype similar to that observed in cells from patients with Dunnigan-type partial lipodystrophy and Emery–Dreifuss muscular dystrophy, Exp. Cell Res. 282 (2003) 14–23.

[24] C. Östlund, G. Bonne, K. Schwartz, H.J. Worman, Properties of lamin A mutants found in Emery–Dreifuss muscular dystrophy, cardiomyo-

pathy and Dunnigan-type partial lipodystrophy, J. Cell Sci. 114 (2001) 4435–4445.

[25] J.L.V. Broers, N.M. Bronnenberg, H.J.H. Kuijpers, B. Schutte, C.J. Hutchison, F.C.S. Ramaekers, Partial cleavage of A-type lamins concurs with their total disintegration from the nuclear lamina during apoptosis, Eur. J. Cell Biol. 81 (2002) 677–691.

[26] D.Z. Fisher, N. Chaudhary, G. Blobel, cDNA sequencing of nuclear lamins A and C reveals primary and secondary structural homology to intermediate filament proteins, Proc. Natl. Acad. Sci. U. S. A. 83 (1986) 6450–6454.

[27] K.M. Wan, J.A. Nickerson, G. Krockmalnic, S. Penman, The nuclear matrix prepared by amine modification, Proc. Natl. Acad. Sci. U. S. A. 96 (1999) 933–938.

[28] B. Schutte, M.M.F.J. Tinnemans, G.F.P. Pijpers, M.H.J.H. Lenders, F.C.S. Ramaekers, Three parameter flow cytometric analysis: simultaneous detection of cytokeratin, proliferation associated antigens and DNA content, Cytometry 21 (1995) 177–186.

[29] B.M. Machiels, J.L. Broers, Y. Raymond, L. de Ley, H.J. Kuijpers, N.E. Caberg, F.C. Ramaekers, Abnormal A-type lamin organization in a human lung carcinoma cell line, Eur. J. Cell Biol. 67 (1995) 328–335.

[30] J.A. Dyer, I.R. Kill, G. Pugh, R.A. Quinlan, E.B. Lane, C.J. Hutchison, Cell cycle changes in A-type lamin associations detected in human dermal fibroblasts using monoclonal antibodies, Chromosome Res. 5 (1997) 383–394.

[31] U. Aebi, J. Cohn, L. Buhle, L. Gerace, The nuclear lamina is a meshwork of intermediate filaments, Nature 323 (1986) 560–564.

[32] L. Gu, J.C. Troncoso, J.B. Wade, M.J. Monteiro, In vitro assembly properties of mutant and chimeric intermediate filament proteins: insight into the function of sequences in the rod and end domains of IF, Exp. Cell Res. 298 (2004) 249–261.

[33] T. Dechat, S. Vlcek, R. Foisner, Lamina-associated polypeptide 2 isoforms and related proteins in cell cycle-dependent nuclear structure dynamics, J. Struct. Biol. 129 (2000) 335–345.

[34] J. Mislow, J. Holaska, M. Kim, K. Lee, M. Segura-Totten, K. Wilson, E. McNally, Nesprin-1alpha self-associates and binds directly to emerin and lamin A in vitro, FEBS Lett. 525 (2002) 135–140.

[35] L. Mounkes, S. Kozlov, B. Burke, C.L. Stewart, The laminopathies: nuclear structure meets disease, Curr. Opin. Genet. Dev. 13 (2003) 223–230.

[36] M. Fricker, M. Hollinshead, N. White, D. Vaux, Interphase nuclei of many mammalian cell types contain deep, dynamic, tubular membrane bound invaginations of the nuclear envelope, J. Cell Biol. 136 (1997) 531–544.

[37] G. Jagatheesan, S. Thanumalayan, B. Muralikrishna, N. Rangaraj, A.A. Karande, V.K. Parnaik, Colocalization of intranuclear lamin foci with RNA splicing factors, J. Cell Sci. 112 (1999) 4651–4661.

[38] P. Hozák, M.-J. Sasseville, Y. Raymond, P.R. Cook, Lamin proteins form an internal nucleoskeleton as well as a peripheral lamina in human cells, J. Cell Sci. 108 (1995) 635–644.

[39] D.A. Jackson, P.R. Cook, Transcriptionally active minichromosomes are attached transiently in nuclei through transcription units, J. Cell Sci. 105 (1993) 1143–1150.

[40] L.C. Mounkes, C.L. Stewart, Aging and nuclear organization: lamins and progeria, Curr. Opin. Cell Biol. 16 (2004) 322–327.

[41] V. Nikolova, C. Leimena, A.C. McMahon, J.C. Tan, S. Chandar, D. Jogia, S.H. Kesteven, J. Michalicek, R. Otway, F. Verheyen, S. Rainer, C.L. Stewart, D. Martin, M.P. Feneley, D. Fatkin, Defects in nuclear structure and function promote dilated cardiomyopathy in lamin A/C-deficient mice, J. Clin. Invest. 113 (2004) 357–369.

[42] P. Sabatelli, G. Lattanzi, A. Ognibene, M. Columbaro, C. Capanni, L. Merlini, N.M. Maraldi, S. Squarzoni, Nuclear alterations in autosomal-dominant Emery–Dreifuss muscular dystrophy, Muscle Nerve 24 (2001) 826–829.

[43] K. Bechert, M. Lagos-Quintana, J. Harborth, K. Weber, M. Osborn, Effects of expressing lamin A mutant protein causing Emery–Dreifuss muscular dystrophy and familial partial lipodystrophy in HeLa cells, Exp. Cell Res. 286 (2003) 75–86.

[44] C. Capanni, V. Cenni, E. Mattioli, P. Sabatelli, A. Ognibene, M. Columbaro, V.K. Parnaik, M. Wehnert, N.M. Maraldi, S. Squarzoni, G. Lattanzi, Failure of lamin A/C to functionally assemble in R482L mutated familial partial lipodystrophy fibroblasts: altered intermolecular interaction with emerin and implications for gene transcription, Exp. Cell Res. 291 (2003) 122–134.

[45] N. Daigle, J. Beaudouin, L. Hartnell, G. Imreh, E. Hallberg, J. Lippincott-Schwartz, J. Ellenberg, Nuclear pore complexes form immobile networks and have a very low turnover in live mammalian cells, J. Cell Biol. 154 (2001) 71–84.

[46] M. Sinensky, K. Fantle, M. Trujillo, T. McLain, A. Kupfer, M. Dalton, The processing pathway of prelamin A, J. Cell Sci. 107 (1994) 61–67.

[47] J.L.V. Broers, B.M. Machiels, H.J.H. Kuijpers, F. Smedts, R. van den Kieboom, Y. Raymond, F.C.S. Ramaekers, A- and B-type lamins are differentially expressed in normal human tissues, Histochem. Cell Biol. 107 (1997) 505–517.

[48] J.A. Dyer, I.R. Kill, G. Pugh, R.A. Quinlan, E.B. Lane, C.J. Hutchison, Cell cycle changes in A-type lamin associations detected in human dermal fibroblasts using monoclonal antibodies, Chromosome Res. 5 (1997) 383–394.

[49] S.V. Strelkov, J. Schumacher, P. Burkhard, U. Aebi, H. Herrmann, Crystal structure of the human lamin A coil 2 B dimer: implications for the head-to-tail association of nuclear lamins, J. Mol. Biol. 343 (2004) 1067–1080.

[50] V. Stierle, J. Couprie, C. Ostlund, I. Krimm, S. Zinn-Justin, P. Hossenlopp, H.J. Worman, J.C. Courvalin, I. Duband-Goulet, The carboxyl-terminal region common to lamins A and C contains a DNA binding domain, Biochemistry 42 (2003) 4819–4828.

[51] J. Lammerding, P.C. Schulze, T. Takahashi, S. Kozlov, T. Sullivan, R.D. Kamm, C.L. Stewart, R.T. Lee, Lamin A/C deficiency causes defective nuclear mechanics and mechanotransduction, J. Clin. Invest. 113 (2004) 370–378.

[52] J.L.V. Broers, E.A.G. Peeters, H.J.H. Kuijpers, J. Endert, C.V.C. Bouten, C.W.J. Oomens, F.P.T. Baaijens, F.C.S. Ramaekers, Decreased mechanical stiffness in LMNA−/− cells is caused by defective nucleo-cytoskeletal integrity: implications for the development of laminopathies, Hum. Mol. Genet. 13 (2004) 2567–2580.

[53] P.F. Davies, K.A. Barbee, M.V. Volin, A. Robotewskyj, J. Chen, L. Joseph, M.L. Griem, M.N. Wernick, E. Jacobs, D.C. Polacek, N. dePaola, A.I. Barakat, Spatial relationships in early signaling events of flow-mediated endothelial mechanotransduction, Annu. Rev. Physiol. 59 (1997) 527–549.

[54] B.R. Johnson, R.T. Nitta, R.L. Frock, L. Mounkes, D.A. Barbie, C.L. Stewart, E. Harlow, B.K. Kennedy, A-type lamins regulate retinoblastoma protein function by promoting subnuclear localization and preventing proteasomal degradation, Proc. Natl. Acad. Sci. U. S. A. 101 (2004) 9677–9682.

[55] M.A. Mancini, B. Shan, J.A. Nickerson, S. Penman, W.H. Lee, The retinoblastoma gene product is a cell cycle-dependent, nuclear matrix-associated protein, Proc. Natl. Acad. Sci. U. S. A. 91 (1994) 418–422.

[56] D.J. Lloyd, R.C. Trembath, S. Shackleton, A novel interaction between lamin A and SREBP1: implications for partial lipodystrophy and other laminopathies, Hum. Mol. Genet. 11 (2002) 769–777.

[57] J.M. Holaska, K.K. Lee, A.K. Kowalski, K.L. Wilson, Transcriptional repressor germ cell-less (GCL) and barrier to autointegration factor (BAF) compete for binding to emerin in vitro, J. Biol. Chem. 278 (2003) 6969–6975.

[58] C. Dreuillet, J. Tillit, M. Kress, M. Ernoult-Lange, In vivo and in vitro interaction between human transcription factor MOK2 and nuclear lamin A/C, Nucleic Acids Res. 30 (2002) 4634–4642.